

# Learning from a large-scale calibration effort of multiple lake temperature models

Johannes Feldbauer<sup>1</sup>, Jorrit P. Mesman<sup>2</sup>, Tobias K. Andersen<sup>3</sup>, and Robert Ladwig<sup>4</sup>

<sup>1</sup>Institute of Hydrobiology, TU Dresden, Dresden, Germany

<sup>2</sup>Department of Ecology and Genetics, Uppsala University, Uppsala, Sweden

<sup>3</sup>National Institute of Aquatic Resources (DTU Aqua), Technical University of Denmark, Kgs. Lyngby, Denmark

<sup>4</sup>Department of Ecoscience, Aarhus University, Aarhus, Denmark

These authors contributed equally to this work.

**Correspondence:** Johannes Feldbauer (johannes.feldbauer@tu-dresden.de) and Jorrit P. Mesman (jorrit.mesman@ebc.uu.se)

**Abstract.** Process-based lake temperature models, based on hydrodynamic principles, are commonly used for simulating water temperature, enabling testing of different scenarios and drawing conclusions about possible water quality developments or changes in important ecological processes such as greenhouse gas emissions. Even though there are several models available, a systematic comparison regarding their performance is missing so far. In this study, we calibrated four different one-dimensional lake temperature models for a global dataset of 73 lakes to compare their performance in reproducing water temperature and we estimated parameter sensitivity for the calibrated parameters. Parameter values, model performance, and parameter sensitivity differed between lake models and between clusters that were defined based on lake characteristics. No single model performed best, with each model performing better than the others in at least some of the lakes. From the findings, we advocate the application of model ensembles. Nonetheless, we also highlight the need to further improve both weather forcing data, individual models, and multi-model ensemble techniques.

## 1 Introduction

The global rise in water temperatures in lakes and reservoirs (O'Reilly et al., 2015; Pilla et al., 2020) is affecting water quality and ecosystem services worldwide in multiple ways; e.g., promoting the formation of harmful cyanobacteria blooms (Huisman et al., 2018), modifying lake ice phenology (Knoll et al., 2019), affecting ecosystem functioning (Kattiel, 2022), or increasing deep-water oxygen depletion (Jane et al., 2023). Water temperature is a “master variable” in aquatic biogeochemical cycling, involved in processes including kinetics of metabolism (Staehr et al., 2010) and greenhouse gas emissions (Audet et al., 2017). Moreover, the vertical temperature structure controls mixing rates between water layers and modifies the position of organisms in the water column as well as the light and nutrient conditions they experience. As such, global future estimates of various water quality and ecological processes in inland waters should be based on an accurate model representation of present and future conditions of lakes temperatures and thermal structures that addresses the variability of lake characteristics worldwide. Recent continental and global-scale modeling efforts have presented convincing evidence of the large impact of climate warming on lake temperatures (e.g. Woolway et al., 2021b; Golub et al., 2022). However, lake models can only be

calibrated for comparatively few lakes for which in-situ, depth-resolved observations exist. Furthermore, there is a knowledge gap on how model performance is affected by different lake-specific characteristics and how models could be parametrized based on the lake characteristics when applied on a global scale. At the moment it is common in global lake modeling studies to apply models without lake- or region-specific calibration (e.g. Woolway et al., 2021a; Vanderkelen et al., 2020) and this adds considerable uncertainty to projections of climate change impacts on lake water temperatures.

Vertical one-dimensional (1D) lake models, based on hydrodynamic principles, are efficient tools to simulate water temperature dynamics for lakes in which the vertical density gradient is more pronounced than the horizontal one. Piccolroaz et al. (2024) gave an extensive review of the theoretical considerations for water temperature modeling across different spatial dimensions and noted the frequent use of 1D models in climate simulations due to their low computational costs and adequate performance. Previous studies have indicated that optimal model parameter values may depend on certain lake characteristics, which could help to obtain more accurate fits in global applications. For instance, an application of the 1D physical lake model GLM (General Lake Model, see Hipsey et al., 2019) with a sensitivity analysis of nine model parameters across multiple lakes suggested that the sensitivity of a subset of parameters depended on characteristics such as lake depth, water transparency, and residence time (Bruce et al., 2018). In a multi-lake application of the 1D physical model ALBM, Guo et al. (2021) highlighted the relationships between the relative influence of model parameters and lake characteristics such as latitude and lake depth. Extending beyond physical variables, Andersen et al. (2021) performed an extensive, global sensitivity analysis on the 1D coupled physical-biogeochemical model GOTM-FABM-PCLake in three Danish lakes and found that in shallow lakes parameter sensitivity may be strongly linked to lake morphology, including a potential feedback of biogeochemical components on temperature (such as light absorption by organic matter).

In this study, we applied four 1D physical lake models to a set of 73 lakes for which in-situ water temperature observations were available, as part of the Inter-Sectoral Impact Model Intercomparison Project (ISIMIP, Golub et al., 2022) using meteorological forcing from bias-corrected reanalysis data. The models were calibrated in a consistent manner, and we report on the overall model performance, highlight consistent patterns in model performance and parameter values, and assessed parameter sensitivity. These calibrations were in preparation for ISIMIP climate impact simulations for the local lakes sector (see Code and data availability). This study approach expands on previous studies through testing the sensitivity of multiple models simultaneously by applying an identical methodology for calibration and sensitivity analysis implemented over a larger number of lakes. Such an in-depth model evaluation on a global scale can:

1. Point towards systematic issues and biases of 1D physical lake models when forced by meteorological reanalysis data.
2. Reveal patterns in model performance driven by geographic location and/or lake characteristics.
3. Test if an optimal model for specific lake types exists, or alternatively, advocate for an ensemble approach.
4. Identify a set of highly sensitive parameters for calibration.

This will expand our knowledge of the accuracy of water temperature modeling on a global scale, improve understanding of the relationship between lake characteristics and model parametrization thus giving advice for practitioners on how to best

calibrate certain lake types, and potentially lead to a more accurate model application. As there is a growing interest in global estimates of water quality and greenhouse gas emissions (e.g., Kakouei et al., 2021; Jansen et al., 2022; Jane et al., 2023; Zhuang et al., 2023), which often rely partially on simulated water temperature and thermal structure, we need to ensure that the underlying global thermal information is as accurate as possible and that the level of uncertainty is known.

## 60 2 Methods

### 2.1 ISIMIP local lakes sector

ISIMIP — the Inter-Sectoral Impact Model Intercomparison Project — is a framework for consistently projecting the impacts of climate change across affected sectors and spatial scales (<https://www.isimip.org>; Frieler et al. (2024)). The Lake Sector is considering the impact of global warming on two categories of lakes: “local lakes” and “global lakes” (Golub et al., 2022).  
65 The “local lakes” were used for this study: 73 lakes for which observed in-situ water temperature data and hypsographic information are available (Table S1 in the Supplementary material). The resolution (vertical and temporal) of the observed data and the detail of the hypsograph varied per lake. For all but two lakes, data covered a period of at least 1 year, and for 75% of the cases it covered at least 5 years. Profiles (three unique depths or more) were provided for all but four lakes, and all lakes had more than 100 unique observations (Figure S1 in the Supplementary material). A link to the observed data and hypsographs is  
70 provided in the Code and data availability statement. No inflow and outflow data are available, so we assumed a constant water level throughout the simulation.

For the forcing of the models we used the GSWP3-W5E5 reanalysis dataset combining the GSWP (Kim, 2017; Dirmeyer et al., 2006) and the W5E5 datasets (Lange et al., 2021; Cucchi et al., 2020). The meteorological forcing, available at daily resolution, for each lake was extracted by the ISIMIP organizational team for the grid cells (spatial resolution: 0.5° by 0.5°)  
75 in which each lake was located (Golub et al., 2022). The following meteorological variables were used to drive the lake simulations: air temperature, relative humidity, precipitation, shortwave radiation, longwave radiation, surface air pressure, and wind speed.

Initial conditions were estimated from observed water temperatures. Therefore, all available data in a period of days (depending on data availability) before and after the start date of the simulation were taken and averaged to set the initial temperature  
80 profile. All simulations used a spin-up period of 1 year.

### 2.2 Lake clustering

In order to analyze the impact of lake characteristics (Table S2 in the Supplementary material) on model performance and parameter sensitivity, we used K-means clustering to group the 73 lakes (Figure 1). Previous to clustering, we log-transformed elevation, mean depth, maximum depth and lake area and applied a z-score transformation. We created a silhouette plot to  
85 determine the optimal number of clusters, which was two. However, we decided to use five clusters instead as this gave a more meaningful representation of different lake types (Figure S2 in the Supplementary material).

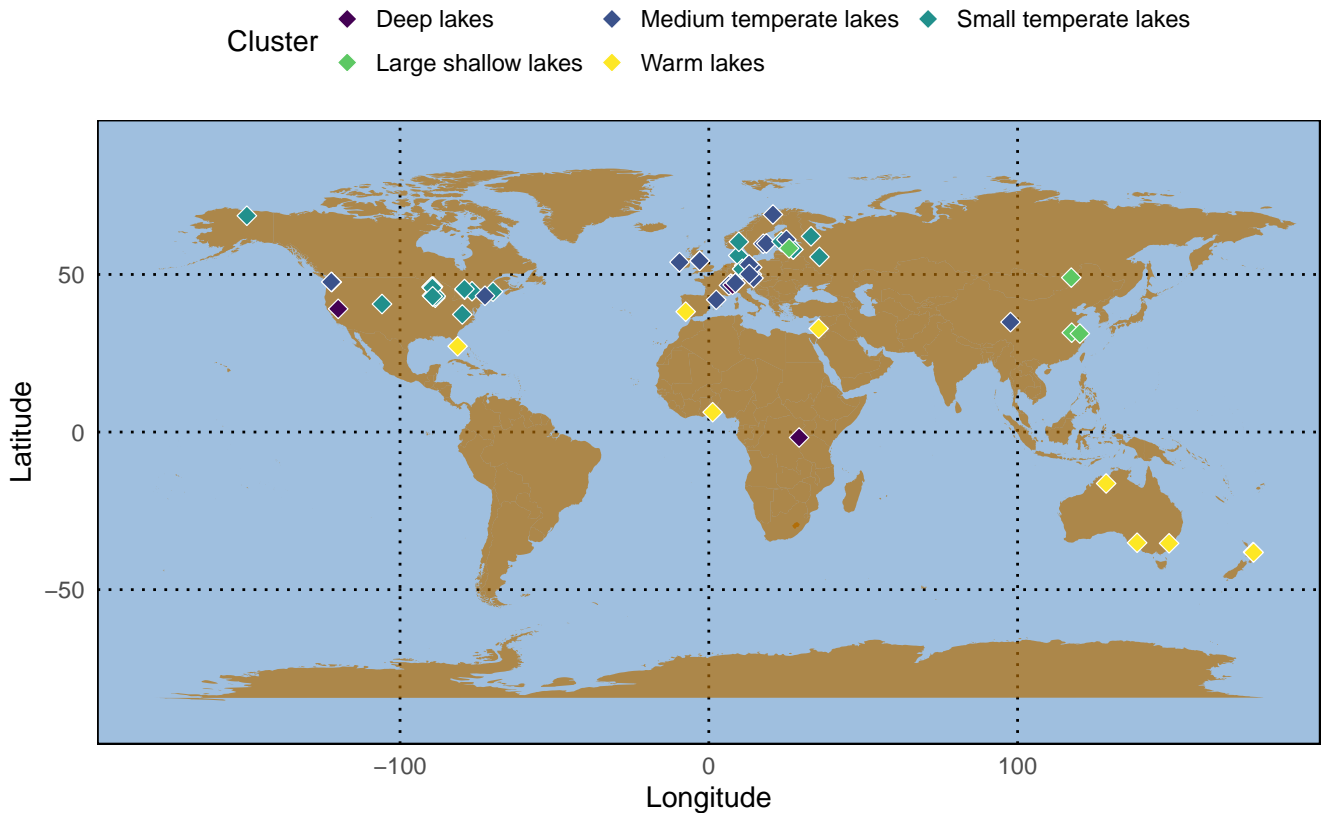


**Figure 1.** Map showing the locations and grouping derived by K-means clustering of the 73 lakes included in the study.

### 2.3 1D physical lake models

Four vertical lake temperature models were used in this study to explore model sensitivity around climate change projections in lakes with varying algorithms and calculations regarding vertical temperature and heat transport: the two-layer (0.5D) model FLake (Mironov, 2008, 2005), the 1D integral energy model GLM version 3.1.0 (Hipsey et al., 2019), the 1D turbulence-based models GOTM lake-branch version 5.4.0 (Burchard et al., 1999; Umlauf et al., 2005) and Simstrat version 2.4.1 (Goudsmit et al., 2002; Gaudard et al., 2019). The models were set up and run using the LakeEnsemblR R-package (Moore et al., 2021) to standardize the approach. We refer to Piccolroaz et al. (2024) for detailed information regarding general concepts in water temperature modeling. In this section we provide a summarized overview of the main differences in process description between these four models. The models were applied in an identical way, with the exceptions that FLake was used to simulate up to the mean depth instead of the maximum depth (in line with assumptions in the model), and that cloud cover was calculated from the meteorological variables using LakeEnsemblR functions for the GOTM model.

The vertical 0.5D (i.e. a box model, but with two separate boxes for upper and lower water layers) lake model FLake was originally designed for weather prediction studies, in which a large-scale climate model is coupled to multiple small-scale lake models. To achieve computational efficiency, FLake simulates the temperature dynamics of an upper completely-mixed layer and a thermocline layer (commonly also known as metalimnion), while neglecting temperature dynamics below the latter one (Mironov, 2005). Vertical temperature evolution itself is parametrized based on the self-similarity concept of the vertical temperature profile (Kitaigorodskii and Miropolsky, 1970). This observed and theoretically-explained concept states that a dimensionless temperature profile in the thermocline can be replicated using a “universal” function of the dimensionless depth  $\zeta$ :

$$\frac{\theta_s(t) - \theta(z, t)}{\Delta\theta(t)} = \Phi_{\theta(\zeta)} \quad (1)$$

where  $t$  and  $z$  are the dimensions over time and depth, respectively. In equation 1,  $\theta_s$  is the absolute temperature of the upper completely-mixed layer,  $\Delta\theta(t)$  is the absolute temperature gradient across the thermocline layer, and  $\Phi_{\theta}$  is the “universal” function of the dimensionless depth. The dimensionless depth can be parametrized as:

$$\zeta = \frac{z - h(t)}{\Delta h(t)} \quad (2)$$

where  $h(t)$  is the depth of the upper, completely-mixed layer, and  $\Delta h(t)$  is the depth difference between the mixed layer depth and the bottom of the metalimnion. Note that in this study, we set the bottom metalimnion depth to each lake’s mean depth. Applying this concept to temperature evolution, FLake parametrizes both layers (upper completely mixed and thermocline layer) as:

$$\Theta = \begin{cases} \theta_s, & \text{if } 0 < z < h \\ \theta_s - (\theta_s - \theta_b) \Phi(\zeta), & \text{if } h \leq z \leq D_{lake} \end{cases} \quad (3)$$

where  $D_{lake}$  is the maximum depth (Mironov, 2005). Similar to the other models, the upper completely-mixed layer receives the energy fluxes from the atmosphere:

$$h \frac{d\theta_s}{dt} = \frac{1}{\rho_w c_w} (Q_s + I_s - Q_h - I(h)) \quad (4)$$

where  $\rho_w$  is water density,  $c_w$  is heat capacity,  $Q_s$  is the turbulent heat flux at the surface,  $I_s$  is the surface short-wave radiative flux,  $Q_h$  is the heat flux from the bottom to the upper layer, and  $I(h)$  is the radiative short-wave flux through the water column (Mironov, 2005). We can state the sum of these individual heat fluxes as the net heat flux exchange  $H_{net}$ . Although FLake’s numerical implementation combines empirical formulations with physical processes, it has demonstrated a good performance for surface water temperature modeling as well as ice phenology investigations (e.g. Mallard et al., 2014) and is commonly applied to global studies (Woolway and Merchant, 2019).

125 GLM, GOTM and Simstrat are vertical 1D lake models in which temperature evolution is quantified at every time step over a vertical grid. Conceptually, the models differ regarding how the vertical grid is configured as GLM applies a flexible structure, whereas the others use a fixed grid with the possibility of refinements. Nonetheless, all three models are based on the vertical water temperature equation, which — in its general form — can be stated as:

$$\frac{\partial T}{\partial t} = \underbrace{-\frac{1}{\rho c_p} \frac{\partial I}{\partial z}}_{(1)} + \underbrace{\frac{H_{sed}}{A \rho c_p} \frac{\partial A}{\partial z}}_{(2)} + \underbrace{\frac{S_T}{\rho c_p}}_{(3)} + \underbrace{\frac{1}{A} \frac{\partial}{\partial z} \left( A D_z^T \frac{\partial T}{\partial z} \right)}_{(4)} \quad (5)$$

130 in which the change of temperature  $T$  over time depends on four terms on the right hand-side: (1) the internal heat generation due to short-wave solar radiation  $I$ , (2) a geothermal heat flux  $H_{sed}$  that acts over an area  $A$ , (3) an internal heat source term  $S_T$ , (4) and a turbulent diffusive term that includes the eddy-diffusivity coefficient  $D_z^T$  (Piccolroaz et al., 2024). The layer adjacent to the atmosphere-water interface receives a net heat flux exchange similar to the one described in equation 4, where  $H_{net}$  is the sum of radiative and turbulent heat fluxes:

$$135 \left. \rho_w c_p \left( D_z^T \frac{\partial T_z}{\partial z} \right) \right|_{z=s} = H_{net} \quad (6)$$

where  $T_z$  is the water temperature of the layer adjacent to the atmosphere-water interface at the surface depth  $s$ .

The main difference between GLM and both GOTM and Simstrat, is how they simulate the turbulent diffusive transport. GLM applies a combination of empirical and physical relationships that use the available external turbulent kinetic energy (TKE) to calculate the thickness of a completely-mixed surface layer (for general information about integral energy models  
140 see Ford and Stefan, 1980). For this, mixing in a surface mixed layer is calculated by comparing the available external energy to the potential energy of the water column that is needed to lift up denser water from below a completely-mixed layer into a newly formed mixed layer until the TKE is no longer sufficient for further mixing (Hipsey et al., 2019). Below the depth of this surface mixed layer, a parametrization for the eddy diffusivity coefficient in relation to water column stability is used to calculate diffusive transport:

$$145 D_z^T = \frac{C_{HYP} \varepsilon_{TKE}}{N^2 + 0.6 k_{TKE}^2 u_*^2} \quad (7)$$

where  $C_{HYP}$  is a constant coefficient for the mixing efficiency (later referred to as the calibration parameter `coef_mix_hyp`),  $\varepsilon_{TKE}$  is a simplified approximation of turbulent dissipation rate based on the dissipation by inflows and wind,  $N^2$  is the squared buoyancy frequency,  $k_{TKE}$  is the turbulence wavenumber, and  $u_*$  is the wind shear velocity (Weinstock, 1981). The buoyancy frequency (Brunt-Väisälä frequency) quantifies local stability to vertical displacements as:

$$150 N = \sqrt{\frac{g}{\rho} \frac{\partial \rho}{\partial z}} \quad (8)$$

where  $g$  is gravitational acceleration.

Simstrat and GOTM are turbulence-based models that apply a two-equation turbulence model to compute the quantities of the production, transport and dissipation rates of TKE. Here, we highlight the  $k - \varepsilon$  two-equation turbulence model which is implemented in both models (Burchard et al., 1999; Goudsmit et al., 2002):

$$155 \quad \frac{\partial k}{\partial t} = \frac{1}{A} \frac{\partial}{\partial z} \left( AD_z^k \frac{\partial k}{\partial z} \right) + P + B - \varepsilon \quad (9)$$

$$\frac{\partial \varepsilon}{\partial t} = \frac{1}{A} \frac{\partial}{\partial z} \left( AD_z^\varepsilon \frac{\partial \varepsilon}{\partial z} \right) + \frac{\varepsilon}{k} (c_{\varepsilon,1}P + c_{\varepsilon,3}B - c_{\varepsilon,2}\varepsilon) \quad (10)$$

where  $D_z^k$  and  $D_z^\varepsilon$  are the turbulent diffusivities of TKE and TKE dissipation, respectively,  $P$  is the TKE production due to shear, and  $B$  is the production and dissipation of TKE related to buoyancy (Rodi, 1984).  $c_{\varepsilon,1}$ ,  $c_{\varepsilon,2}$  and  $c_{\varepsilon,3}$  are empirical constants. In GOTM, whenever the simulated TKE is lower than the calibration parameter `k_min`, it is set to the value of `k_min`. We can compute the eddy diffusivity coefficient  $D_z^T$  as a function of the turbulence kinetic energy  $k$  and dissipation rate  $\varepsilon$ :

$$D_z^T = \frac{c_\mu k^2}{\sigma_t \varepsilon} \quad (11)$$

where  $c_\mu$  is an empirical coefficient, and  $\sigma_t$  is the turbulent Prandtl number.

165 Simstrat further employs an empirical seiche excitation and damping model to improve the representation of internal seiches in transport processes (Goudsmit et al., 2002). Here, seiche movement can produce additional TKE,  $E_{seiche}$ , inside the water column with the intention to provide a more realistic simulation of vertical transport due to bottom boundary mixing as seiche motion damping acts as an energy source below the mixed layer:

$$\frac{dE_{seiche}}{dt} = \underbrace{\alpha A_0 \rho_{air} c_{10} (u_{10}^2 + v_{10}^2)^{3/2}}_{PW} - \underbrace{C_{Def f} A_0 V^{-3/2} \rho_0^{-1/2} E_{seiche}^{3/2}}_{LS} \quad (12)$$

where  $PW$  is energy production,  $LS$  is energy loss,  $\alpha$  is a model parameter to describe the wind energy fraction that is transferred to the seiche motion (later referred to as the calibration parameter `a_seiche`),  $c_{10}$  is the drag coefficient,  $u_{10}$  and  $v_{10}$  are velocity components of wind speed measured at 10 m above water surface, and  $C_{Def f}$  is the effective bottom friction coefficient (Goudsmit et al., 2002). We note that similar algorithms, designed to improve vertical mixing dynamics below the epilimnion, exist also in other models, including integral energy models, i.e., the turbulent benthic boundary layer mixing algorithm by Yeates and Imberger (2003), but are not — to the best of our knowledge — implemented in GLM and GOTM.

175 An additional structural difference between the models is their process description of the treatment of attenuation of short-wave radiation, especially the non-visible near-infrared light (NIR) and the visible parts of short-wave radiation. FLake does not distinguish between these parts of the light spectrum, and applies the Beer-Lambert law for light attenuation with depth (see also Stepanenko et al., 2014, for a more detailed analysis), although the model can be parametrized to consider a set of different

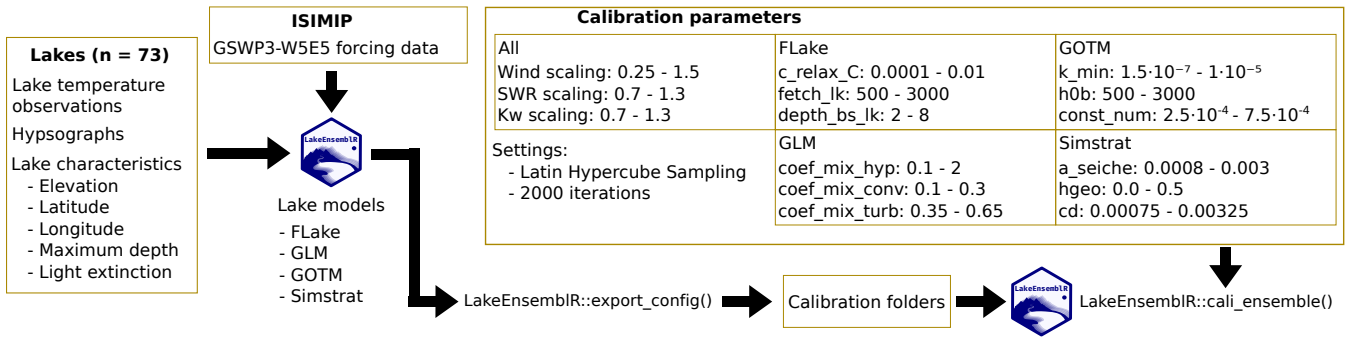


**Figure 2.** Workflow of the calibration, for a description and units of the calibrated parameters see Table 1. The light extinction coefficient ( $K_w$ ) was calibrated 30% around the default value for each specific lake.

wavelength bands with variable attenuation coefficients (Mironov, 2005). GLM has the option to apply the Beer-Lambert law for only the photosynthetically active fraction (PAR), while the NIR and ultraviolet bandwidths are attenuated directly in the layer adjacent to the atmosphere-water interface (Hipsey et al., 2019). A second option in GLM uses the algorithm by Cengel and Ozisk (1984) to simulate light penetration of individual bandwidth fractions. However, in this study the first option was applied which treats 45% of the incoming short-wave radiation as PAR which subsequently is attenuated in the layers below the atmosphere-water interface. Similarly, GOTM was configured to have a separate depth-specific attenuation for the visible and non-visible light fractions. In this study, the incoming short-wave radiation was split into non-visible and visible fraction with 55% and 45%, respectively. The light extinction coefficient for non-visible light was set to  $2 \text{ m}^{-1}$ . Although Simstrat does not split light into separate fractions, it uses a parameter to absorb a fixed fraction of short-wave radiation (in this study set to 30%) in the uppermost water layer, eventually resulting in a similar impact of fast absorption of a part of the solar energy near the atmosphere-water interface (see also Gaudard et al., 2019). This highlights that potentially more heat gets absorbed in the layer adjacent to the atmosphere-water interface in the GLM, GOTM, and Simstrat simulations than in the FLake simulations.

## 2.4 Calibration workflow

The workflow (Figure 2) to calibrate the models for the 73 lakes is described in the following section. For each lake we gathered the available data from ISIMIP: observed water temperatures, lake hypsography, lake location (elevation, coordinates), and light extinction (or Secchi disk depth data to derive light extinction). Observed water temperature data with subdaily resolution were averaged to daily mean values. If no data on the light extinction were available, we estimated it from Secchi disk depth (Koenings and Edmundson, 1991). If no Secchi disk depth was available as well, we estimated it from the maximum lake depth (Håkanson, 1995). We then formatted the ISIMIP data to a pre-defined standard format, from which the LakeEnsemblR package (Moore et al., 2021) generated model-specific forcing and configuration files. We used four lake models included in LakeEnsemblR (GLM, GOTM, Simstrat, and FLake) which are described in Section 2.3.



**Table 1.** Description of the calibrated parameters. For the range of the parameters see Figure 2

Parameter	Unit	Description	Model
wind_speed	-	Scaling factor for wind speed	All models
swr	-	Scaling factor for incoming shortwave radiation	All models
Kw	1/m	Scaling factor for estimated light extinction	All models
c_relax_c	-	Constant in relaxation equation of shape factor	FLake
fetch_lk	m	Typical wind fetch	FLake
depth_bs_lk	m	Depth of thermally active layer in bottom sediments	FLake
k_min	m <sup>2</sup> /s <sup>2</sup>	Minimum turbulent kinetic energy	GOTM
h0b	m	Physical bottom roughness length	GOTM
const_num	m <sup>2</sup> /s	Constant eddy diffusivity	GOTM
coef_mix_hyp	-	Mixing efficiency of hypolimnetic turbulence	GLM
coef_mix_conv	-	Mixing efficiency of convective overturn	GLM
coef_mix_turb	-	Mixing efficiency of unsteady turbulence effects	GLM
a_seiche	-	Fraction of wind energy that goes to seiche energy	Simstrat
hgeo	W/m <sup>2</sup>	Geothermal heat flux	Simstrat
cd	-	Bottom drag coefficient	Simstrat

200 Finally we ran the calibration using a latin hypercube approach (see e.g. Mckay et al., 2000). Here, we chose 6 parameters for each model: three model-specific parameters, and three scaling factors (for wind speed, incoming shortwave radiation, and the estimated light extinction coefficient, respectively; Table 1). For the model-specific parameters, we chose parameters that are commonly used to calibrate these models, based on literature (see Moore et al., 2021) and personal communication with model users. We sampled and ran the four models for 2000 parameter sets, and for each of the parameter sets we calculated  
205 four performance metrics over all water temperature observations: Root mean squared error (RMSE), Nash-Sutcliffe model efficiency (NSE), Pearson correlation coefficient (R), and mean error (bias)

## 2.5 Global sensitivity analysis

Based on the sampled parameter sets and the calculated performance metrics, we performed a Delta Moment-Independent sensitivity analysis (Plischke et al., 2013; Borgonovo, 2007) for each performance metric per lake per model, using the Python  
210 library SALib (Iwanaga et al., 2022; Herman and Usher, 2017). The analysis calculates two sensitivity measures, the moment-independent  $\delta$  and variance-based Sobol  $S1$ . The delta moment-independent measure  $\delta$  considers the entire distribution of model output instead of a particular moment (e.g., variance) by calculating the difference between unconditional and conditional cumulative distribution functions of the simulated model output, whereas the variance-based first-order sobol index  $S1$  calculates a parameter's influence on the variance of the simulated model output (Plischke et al., 2013; Borgonovo, 2007).  
215 As this study was interested in identifying the most important parameters (i.e. factor prioritization setting), we followed the

recommendations of (Borgonovo et al., 2017) and used both variance-based and moment-independent measures to increase the robustness when inferring which parameters are most important when simulating water temperatures. In addition to the six calibrated parameters, we included a dummy parameter that had no influence on the model output in the sensitivity analysis, which we sampled from a uniform distribution ranging from 0 to 1. In theory, this dummy variable should have a sensitivity of zero, but due to the numerical approximation of the sensitivity measures it can have small non-zero values. This can be used to approximate the error of estimating sensitivity indices and thereby avoid classifying non-influential parameters as influential. This approach has been used in previous studies (e.g. Andersen et al., 2021; Khorashadi Zadeh et al., 2017). A resample size of 100 was used to compute confidence intervals on both sensitivity analysis metrics. To provide an estimate of potential parameter interactions, we additionally calculated the interaction indicator  $S_{interaction}$  (Borgonovo et al., 2017; Saltelli et al., 2000) that describe the fraction of model output variation apportioned by interactions:

$$S_{interaction} = 1 - \sum_{i=1}^k S_i \quad (13)$$

where ( $S_i$ ) is the first-order variance-based sensitivity measure ( $S1$ ) of parameter  $i$  out of  $k$  tested parameters.

### 3 Results

#### 3.1 Model performance

The single best performing model (out of the four applied models) for each lake reproduced observed water temperatures well for all 73 lakes, with a median RMSE of 1.2 °C and a median R of 0.98 (Figure 3). The variation in error metrics between best and worst performing model for each lake was rather small, e.g. a standard deviation of 0.5 °C or less in RMSE (Figure S3 in the Supplementary material). Simstrat performed the best in most lakes in terms of RMSE, R, and NSE, while GLM performed best in most lakes for bias (Figure 3). However, all four models outperformed the others in at least some of the lakes. In over 90% of all lakes at least two different models performed best for different metrics.

Following the cluster analysis, we classified the lakes into five clusters. We visually compared the characteristics of the clusters (Figure S4 in the Supplementary material) and characterized them according to their most noticeable features: “deep” (n = 3), “medium temperate” (n = 25), “small temperate” (n = 32), “large shallow” (n = 4), and “warm” lakes (n = 9) (Figure 1). Model performance was comparable between the cluster, although the “deep” lakes had a lower RMSE while “medium”, “small temperate”, and “large shallow” lakes performed best in terms of NSE and R (Figure S5 in the Supplementary material). When considering the four models separately, the overall better performance of Simstrat was mostly due to its better performance in the “deep” and “medium temperate” lakes, compared to the other models. In the other three clusters the four models performed similarly (Figure S6 in the Supplementary material).

We calculated the ensemble mean by taking the arithmetic mean of the four models for each time step and depth individually. We then tested this as an additional predictor for water temperature and calculated its performance in terms of RMSE. For the

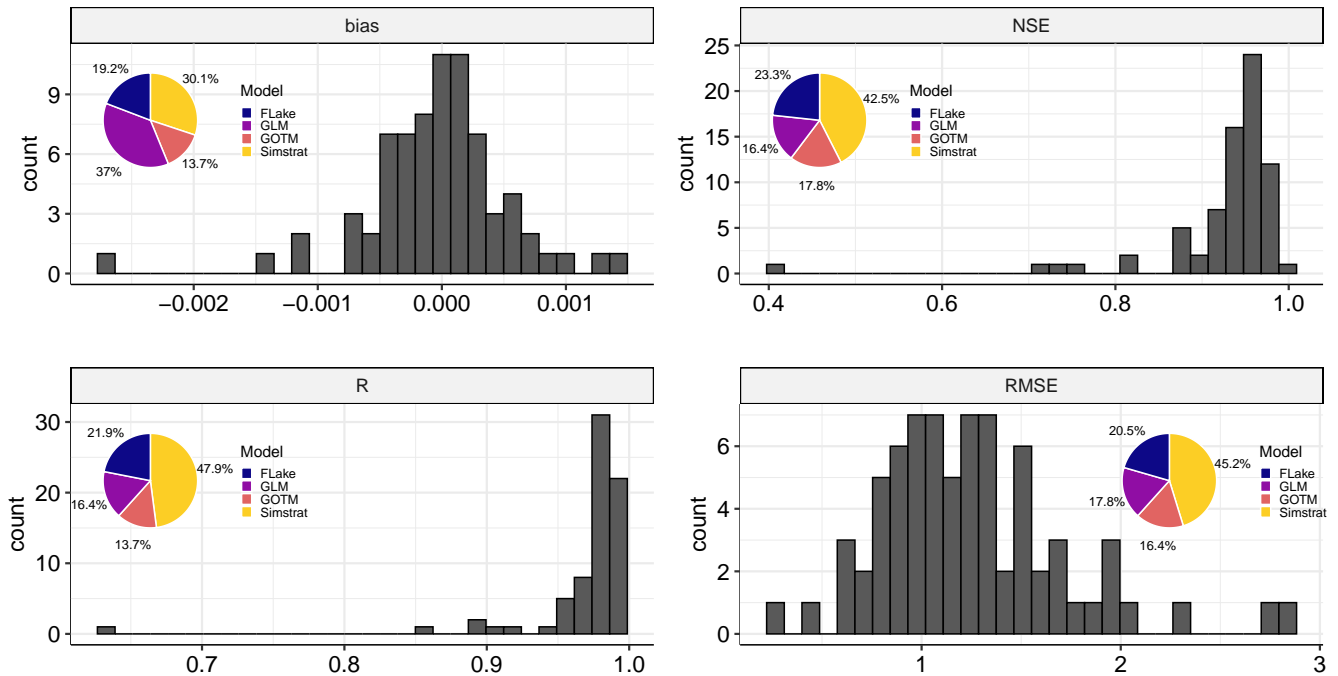


**Figure 3.** Distribution of the six evaluated performance metrics for the single best performing model over the 73 lakes. The pie charts show how often the different models performed best per lake and metric. The unit of RMSE and bias is  $^{\circ}\text{C}$

majority of lakes, the ensemble mean performed better than any single model (Figure S7 in the Supplementary material). This is especially visible in the “medium temperate”, “small temperate”, and “large shallow” lakes where the ensemble mean performed best for the majority of lakes. The cases where the ensemble mean did not perform better than each single model were often lakes in which a single model performed notably better or worse than the other three models.

250 Looking at the distribution of the model error in terms of RMSE over the water column depth (Figure 4 A), we can see that for the “medium temperate” lakes, Simstrat performed better over all depths. In the “deep” lakes, FLake performed considerably worse than the other three models, especially at intermediate depths. For the other three models, the error was increasing towards the surface. For all four models in the “large shallow” lakes the error was larger at the surface, while for the “warm” lakes the error was largest in the intermediate depths.

255 From the observed water temperatures, we calculated the thermocline depth and then chose the simulation–observation pairs closest to that depth to estimate the RMSE at the thermocline temperature (Figure 4 B). For the “large shallow” lakes, no thermocline could be calculated. Simstrat performed best at the thermocline depth for “deep”, “medium temperate”, and “warm” lakes, whereat the performance in “deep” and “medium temperate” lakes was about  $0.5^{\circ}\text{C}$  better, while for “warm” lakes it was only about  $0.1^{\circ}\text{C}$  lower than the next best model. For “small temperate” lakes GLM performed better with an

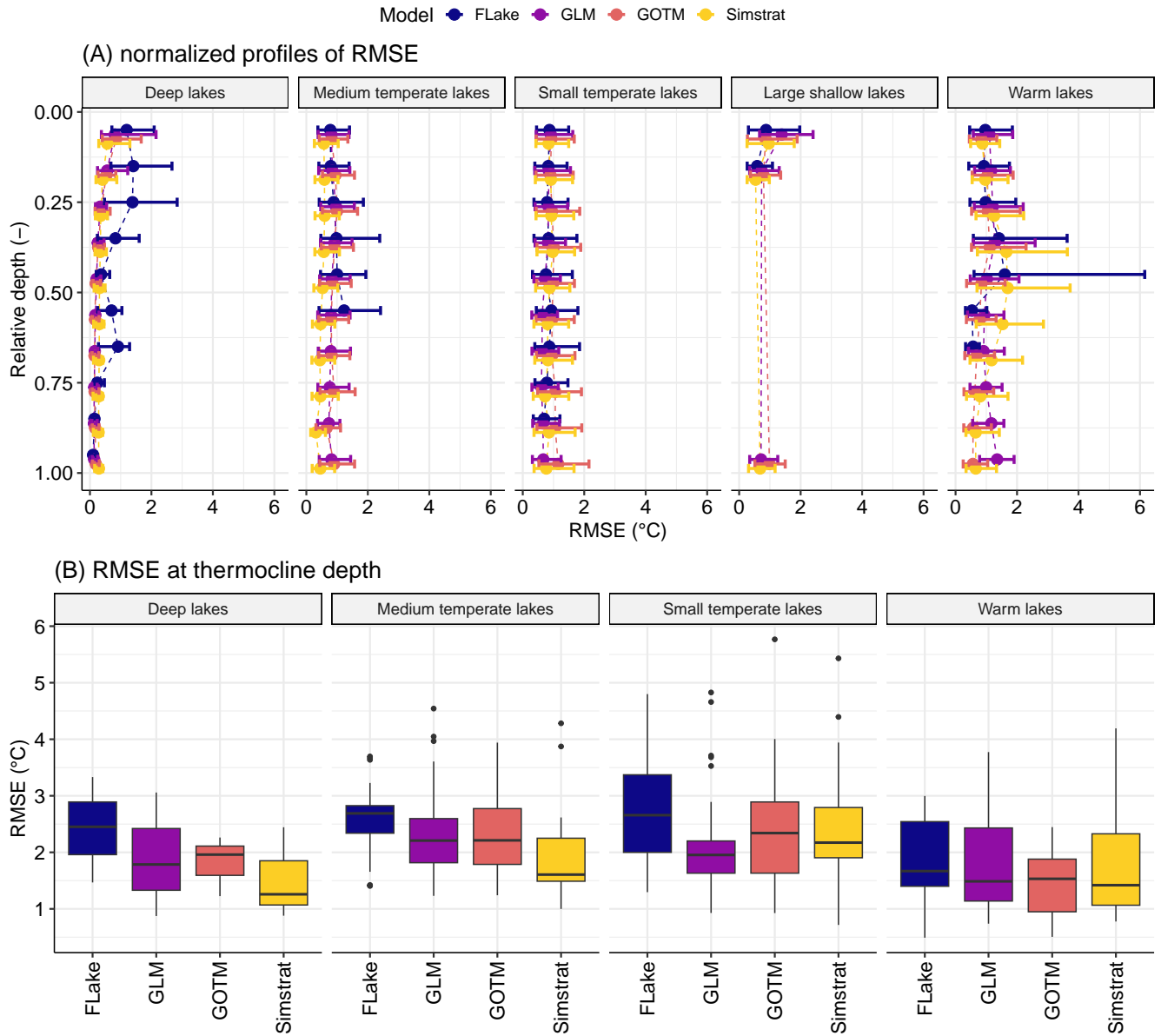


**Figure 4.** Depth distribution of the root mean squared error (RMSE) for the models and lake clusters (A) and boxplots of RMSE at the thermocline depth (B). The depth was normalized to the depth of the deepest measurement (0 being surface and 1 being the deepest point) and then binned in steps of 0.1. The points represent the median RMSE over all profiles and the error bars the 25% to 75% quantiles. If water temperatures deeper than 3 meter were unavailable, no thermocline was calculated.

260 median RMSE about 0.3 °C lower than the next best model. FLake performed poorest at the thermocline depth in all lake cluster.

### 3.2 Parameter sensitivity

From the calibration runs using the latin hypercube approach, we calculated moment-independent measure  $\delta$  and variance-based first-order measure  $S1$  for each combination of models, performance metrics, and lakes (Figure 5). We saw similar  
265 ranking of most influential model parameters on most combinations of models, performance metrics, and lakes for  $\delta$  and  $S1$ . For almost all lakes, the same 3 – 4 parameters were classified as sensitive: the scaling factors for wind speed, shortwave radiation, and light extinction as well as  $k_{min}$  for GOTM. Moreover, 1 or 2 of these parameters accounted for more than 75% of the sum of the sensitivity measures for most lakes (Figure S8 in the Supplementary material). Most often these were meteorological scaling factors, that are not model specific, with the exception of GOTM, in which  $k_{min}$  was most sensitive.  
270 Additionally, the light extinction coefficient and other model-specific parameters appeared to be sensitive in a couple of lakes (Figure 5), but to a lesser degree.

For most models and performance metrics, interaction effects accounted for less than 20% of variation in model performance, though interactions were relevant for specific models and lake groups (Figure 6). For instance, interactions were relevant for GLM modeling “deep” lakes and to a lesser degree GLM and Simstrat modeling “large shallow” lakes. In contrast, increased  
275 parameter interactions were observed for FLake, especially for NSE and RMSE, for all lake clusters except “deep” lakes. We highlight that especially in lakes with shorter time series of observed water temperature data, the interaction measure was larger (Figure S9 in the Supplementary material). Interactions were low for bias for all models and lake clusters.

### 3.3 Distribution of best parameter values

Looking at the parameter values from the best performing parameter sets, the optimal meteorological scaling factors differed  
280 between models. Especially GOTM showed a different behavior from the other models, with lower wind speed scaling factors and a higher shortwave radiation scaling factor (Figure 7). The lake clusters also differed in the optimal scaling factors, though their effects seemed model-specific. Differences in extinction factor scaling were less clear than the meteorological scaling factors, but GLM preferred a higher extinction factor in “large shallow” lakes, and FLake a higher extinction factor in “deep” and “medium temperate” lakes. Most model-specific parameters had a low sensitivity, but some still showed markedly different  
285 behavior between cluster (Figure S10 in the Supplementary material). The single model-specific parameter with high sensitivity, GOTM’s  $k_{min}$ , had distinctly lower values in “small temperate” lakes. Both for the scaling factors and the model specific parameters, we saw that depending on which performance metric was used to select the best parameter set, the outcome was different (see Figure S11 in the Supplementary material).

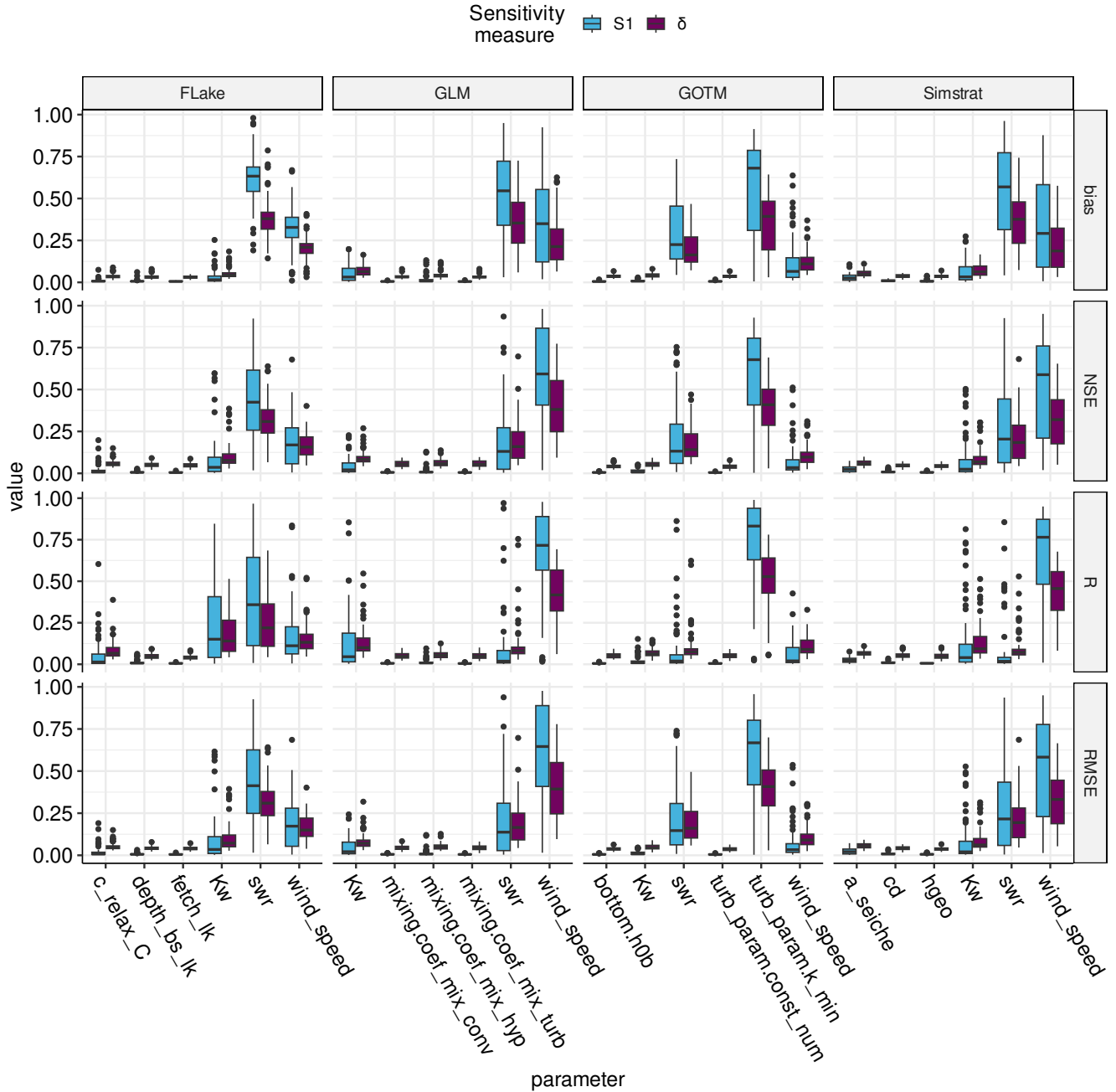


**Figure 5.** Boxplot of the two calculated sensitivity measures for each parameter of the four models and for the four calculated performance metrics over all lakes.

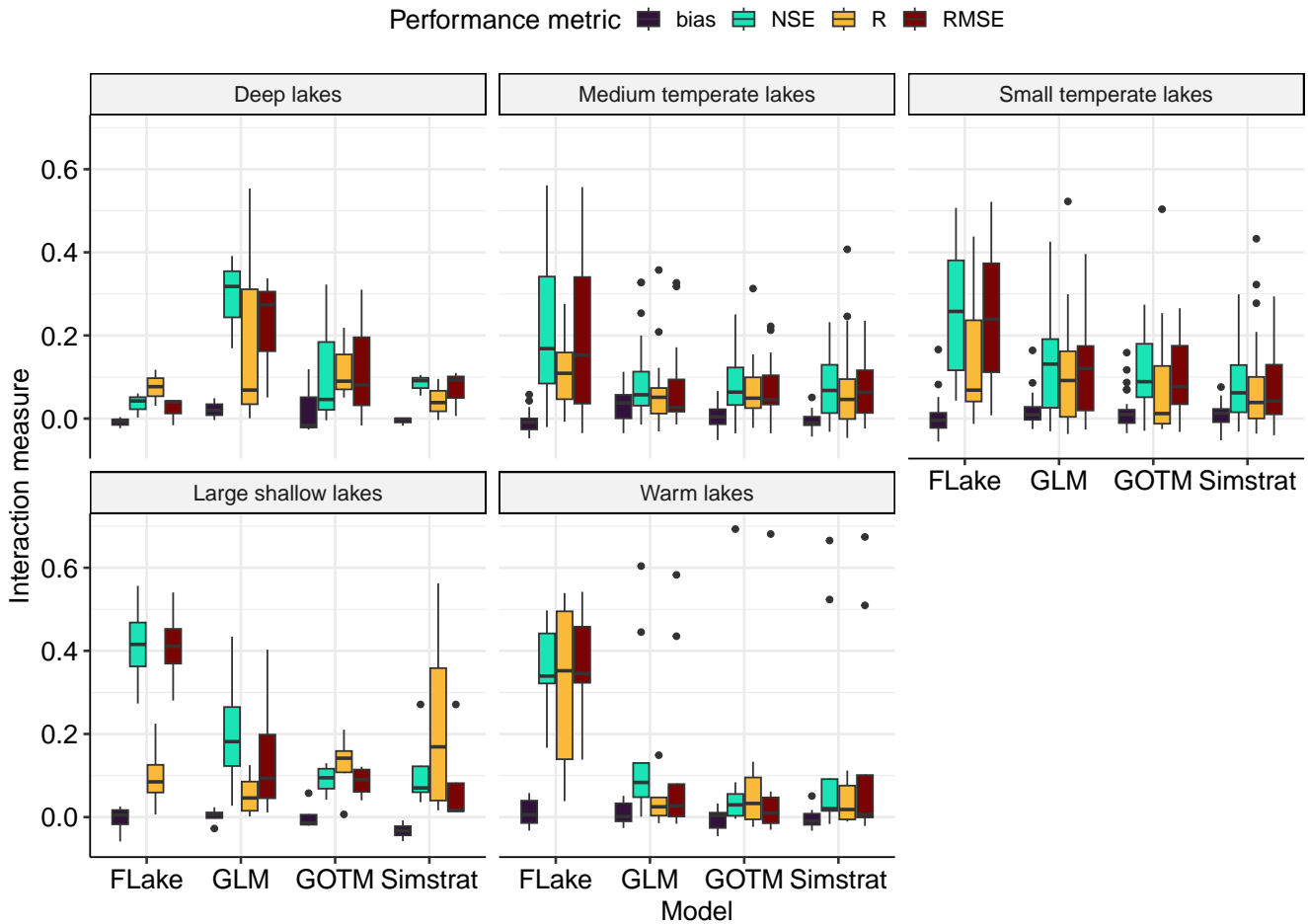


**Figure 6.** Boxplot of the interaction measure of first order sensitivity metric for the four models and performance metrics over all lakes.

#### 4 Discussion

290 Using a standardized and computationally efficient calibration approach (2000 model runs per model and lake) we were able to reproduce water temperature to a sufficient accuracy for 73 lakes across the globe. For 95% of the lakes, the single best performing model had an RMSE below 2 °C with a median of all performing models at 1.2 °C. Model-specific performance (Table S3 in the Supplementary material) naturally showed higher error values but remained below 2 °C for most lakes and models. Compared to a previous ISIMIP simulation round, the performance in terms of median RMSE was similar (ISIMIP 2b, 295 Golub et al., 2022), although in our simulation, GLM, GOTM, and Simstrat performed slightly worse and FLake slightly better. Possible reasons for this could be the different meteorological forcing, the composition of lakes, and a different calibration approach. In comparison to two other multi-lake applications of gridded meteorological data, our calibration performed similar

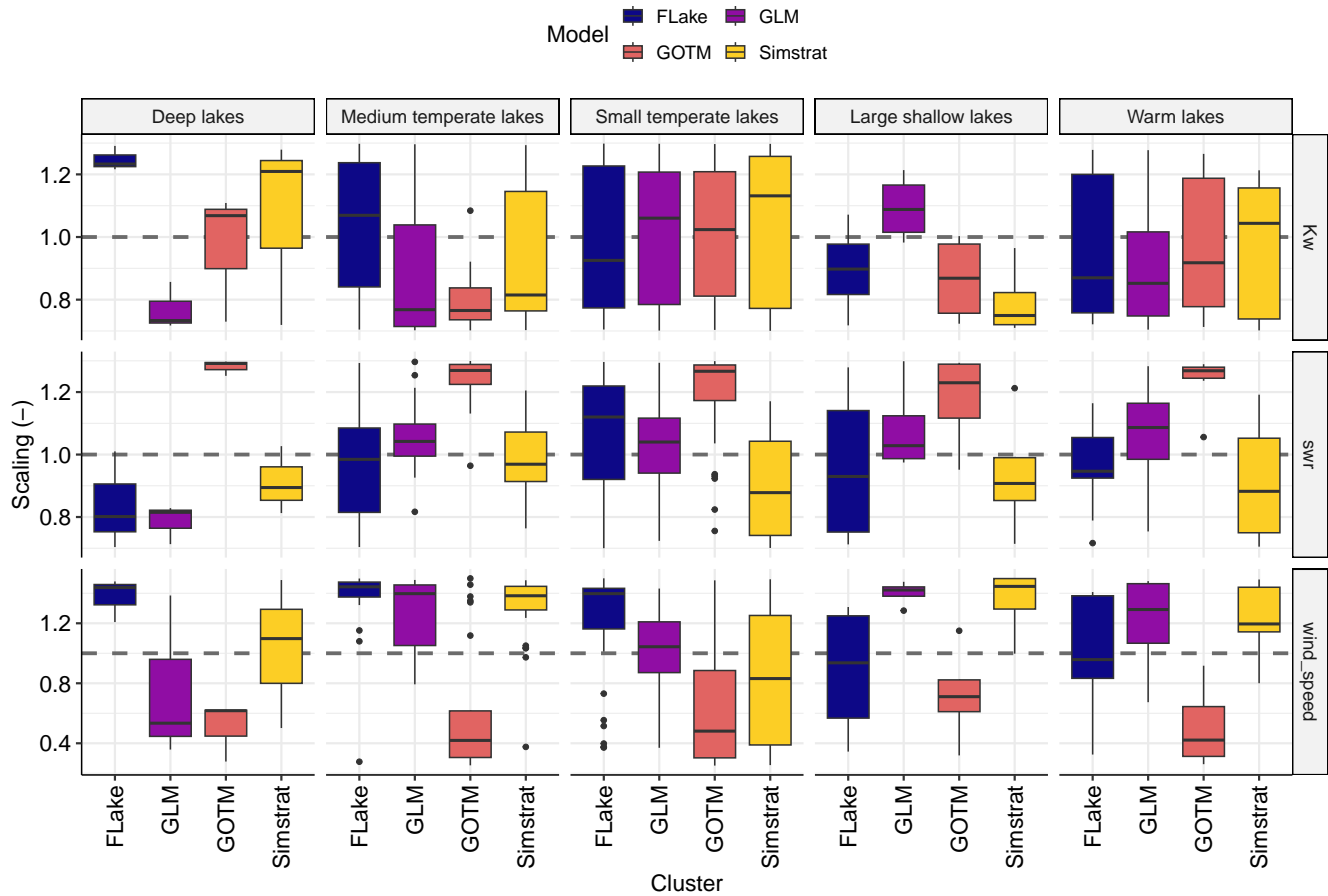


**Figure 7.** Distribution of the wind speed, shortwave radiation (swr), and light extinction (Kw) scaling factors, faceted by model and lake clusters. The light extinction scaling factors are normalized to each lake’s default light extinction value. The optimal values are determined only based on RMSE.

(ALBM, Guo et al., 2021) or better (GLM, Read et al., 2014) in terms of RMSE. In over 40% of all lakes, the ensemble mean performed better than any single model in terms of RMSE. Similar to previous studies using an ensemble framework  
 300 (e.g. Feldbauer et al., 2022; Ladwig et al., 2023), it seems that the ensemble mean is a good predictor for water temperature dynamics. However, when using a larger global dataset, we showed that for a subset of lakes using the simple arithmetic average as an ensemble mean did not increase performance. As in many of these cases a single model performed notably better or worse than the other ensemble members, so a step forward could be to use other averaging techniques to make better use of the ensemble simulation. Such approaches already exist in other fields, like the reliability ensemble averaging method (REA)  
 305 for climate simulations (Giorgi and Mearns, 2002).



Model performance showed a distinct pattern over the five lake clusters: when looking at RMSE, general model performance in “deep” lakes was better, while in “large shallow” lakes it was worse compared to the other clusters. But, both “deep” and “warm” lakes showed poorer model performance when considering NSE (Figure S5 in the Supplementary material). We attribute the model performance in “deep” lakes ( $n = 3$ ) to the low variation in the deep water temperatures, which the models could approach closely (low RMSE), whereas the relatively small temporal variations were harder to simulate (i.e. poorer performance in terms of NSE). The reduced model performance in terms of RMSE for “large shallow” lakes ( $n = 4$ ) was likely due to the intense interaction with the atmosphere (worsened by the use of gridded instead of locally observed meteorological data), while the lower NSE in “warm” lakes ( $n = 9$ ) can be explained by the reduced seasonality in weather forcing data, and thus a harder-to-achieve high performance in metrics relying on temporal trend. Other performance differences between lake clusters, such as in bias, or any differences between the two largest clusters (“small temperate” and “medium temperate” lakes) were marginal. These two largest clusters covered 78% of the lakes in the dataset, which is in line with the higher presence of temperate lakes in the ISIMIP dataset. However, the unequal division of lakes over the clusters does skew the comparison as drawing conclusions regarding differences in other clusters are based on lower sample sizes.

To discuss how individual model performance is related to the underlying equations and design, we first need to acknowledge limitations of this analysis: (a) parameter selection was limited and had identical ranges across models, which could cause a bias for models that would need specific adjustments during calibration, and (b) we neglected any inflows and outflows. Observed water temperature fluctuations caused by entrainment or withdrawal could be apparent in the training data and models could replicate them by manipulating other processes (internal shear or mixing), thereby neglecting the actual hydrodynamic flow processes which caused the above-mentioned temperature fluctuations. We note that the level of complexity in the process formulations for inflows and outflows varies across the models. Putting these caveats due to the standardized methodology aside, 1D lake models have an improved performance compared to the single 0.5D lake model, like FLake, for “deep” and “medium temperate” lakes. Here, all 1D lake models better replicated water temperatures in the surface layers (relative depths up to 0.75 and about 0.5 for “deep” and “medium temperate lakes”, respectively, Figure 4 A) underscoring that their respective algorithms, wind-induced mixing in GLM and computation of TKE in GOTM and Simstrat, outperforms the shape assumptions that underlie FLake to replicate depth-specific near-surface water temperature dynamics. Additionally, their higher light extinction near the atmosphere-water surface due to attenuation of non-visible light could also be a factor in their improved depth-specific simulation of water temperature in “medium temperate” and “deep” lakes. Below the epilimnion, at the thermocline, Simstrat outperforms the other models (Figure 4 B) in “deep” and “medium temperate” lakes. This underscores the importance of accounting of energy sources below the epilimnion. We assume that Simstrat’s seiche excitation and damping parametrization has more accurately simulated the availability of TKE at these metalimnetic depths, which were not reached by wind shear stress originating from the atmosphere-water interface. We reinforced this hypothesis by performing additional simulations with `a_seiche` set to 0, which lead to poorer model performance of Simstrat (see Supplementary material for details). This emphasizes the importance of implementing deep-water mixing algorithms in 1D lake models to account for mixing at intermediate depths, which are usually characterized as quiet regarding turbulent fluxes (Wüest and Lorke, 2003). In the

340 hypolimnion, models performed similarly, with Simstrat only producing slightly better replications of deep-water temperature in “medium temperate” lakes.

For the calibration of the lake models we took an approach commonly used in applied studies where scaling factors for wind speed and shortwave radiation, the extinction coefficient, and a few model-specific parameters are calibrated (e.g. Ayala et al., 2020; Weber et al., 2017). Additionally, we used the output of the calibration to conduct a global sensitivity analysis  
345 of the calibrated parameters. We selected the model-specific parameters and the ranges for all parameters based on previous studies and expert knowledge, but acknowledge that this approach is somewhat limited compared to an extensive sensitivity analysis including all model parameters. However, to our knowledge there are only a few studies looking at the sensitivity of the parameters of the used models (e.g., GLM - Bruce et al., 2018; GOTM - Andersen et al., 2021) and even those did not include all model parameters. Moreover, the model performance of all four investigated performance metrics was comparable to  
350 similar studies (e.g. Golub et al., 2022), despite using only a selection of parameters for the calibration. The sensitivity analysis revealed that for most lakes and models, the most sensitive parameters were the scaling factors. So, it could be reasoned that for similar applications only calibrating the scaling factors could be sufficient. The clear exception here is GOTM, for which minimum turbulent kinetic energy level ( $k_{min}$ ) showed to be highly sensitive for all lake clusters besides the large shallow lakes (Figure S12 in the Supplementary material). In fact,  $k_{min}$  was so important that it could dominate the other scaling  
355 factors leading to different overall patterns in the calibrated parameters with lower values for the wind speed scaling across all lakes, compared to the other models (Figure 7). This warrants future caution when calibrating  $k_{min}$  as this parameter, which directly manipulates background turbulent kinetic energy and therefore turbulent transport, is highly sensitive. A way forward to address this could be to use local field measurements to restrict the lake-specific range of estimates for  $k_{min}$ .

Especially the range for the wind speed scaling which we used in the calibration was quite large (0.25 - 1.5) and even with  
360 this range for some of the lakes the best performing estimates are located close to the limits. An explanation for this large range of scaling factors is that we used forcing from bias-corrected (to global data sources, not data measured above the lakes, Lange (2019)) reanalysis data with a grid size of  $0.5^\circ \times 0.5^\circ$ . Local wind fields can have large variations and especially for lakes, sheltering plays an important role, as lakes are by definition located in depressions in the landscape. Simultaneously, larger lakes can act as smoother surfaces with higher near-surface wind speeds compared to surrounding areas. We could not highlight  
365 any relations between best parameter values for wind speed scaling factors and lake size, which could imply that the gridded weather data mask any effects of lake size. This highlights that there is still potential for enhancement in model quality of local wind speed (Tan et al., 2024). The use of daily-aggregated wind speeds also requires caution, as the mechanic energy transferred to the water is a cubic function of wind speed (Wüest et al., 2000), and therefore averaging of the measured wind speed can lead to underestimation of mixing. The large range for the wind speed (and shortwave radiation) scaling factors were probably  
370 partly responsible for their high sensitivity. In a setting with locally observed meteorological forcing data, the model-specific parameters might become more influential, if meteorological forcing variables can be better constrained. Previous studies used this approach in one or a few lakes (e.g. Guseva et al., 2020; Guo et al., 2021), but it would be beneficial to compile such data for a larger number of lakes, similar to the present study. Reducing the strong influence of meteorological scaling factors could facilitate identification of optimal models for different clusters. If observations are not available, improvements in downscaling

375 methods from global products to weather conditions at the lake surface might also partially achieve this. Similarly, use of hourly meteorological forcing could result in more realistic patterns in wind-driven or convective mixing (Ayala et al., 2020).

We highlight that both sensitivity metrics and calibrated parameter values were strongly influenced by the chosen performance metrics (see e.g. Figure 5 and Figure S11 in the Supplementary material). This means that depending on which performance metric is chosen, the model configuration would be different (except for RMSE and NSE, which will lead to the same set of parameters). Therefore, it is important to choose the model performance metric with care as they capture different aspects of the performance (see e.g. Jachner et al., 2007). For a more thorough assessment of the choice of performance metrics, model validation at multiple levels of complexity could be performed (Hipsey et al., 2020).

Interaction between parameters was larger for FLake specifically, and for GLM in “deep” and for GLM and Simstrat in “large shallow” lakes (Figure 6). For the lakes with high interaction measures, we found interdependence of two or more parameters, most notably wind speed scaling and shortwave radiation scaling, in some cases also the light extinction factor or model-specific parameters. A higher shortwave radiation increases near-surface water temperatures and can promote stratification, while a higher wind speed has largely the opposite effect. The effect of wind on mixing dynamics is notably different, so that given enough observations, the influence of the two variables can be separated. We could see that with lakes that had longer time series of observed water temperature, the interaction measure was generally lower for GLM, GOTM, and Simstrat (Figure S9 in the Supplementary material). Though for the simpler temperature algorithms in FLake, separating the impact of wind speed and shortwave radiation seems to be more difficult. Similarly, the lake type (identified by the clustering) seemed to influence the degree of interaction as well, perhaps extending to other parameters than meteorological scaling factors, which is in line with the findings of Andersen et al. (2021).

The overall uncertainty of mechanistic simulations is usually related to uncertainty in the initial conditions, uncertainty in the driving data (both forcing data such as meteorology and data used for calibration such as water temperature), uncertainty in the model parameter values, and structural uncertainty in the process description also called epistemic uncertainty (Thomas et al., 2020; Scavia et al., 2021; Dietze, 2017). In this study, we aimed at exploring the relationships between lake model performance, parametrization, and lake characteristics. For this, our main focus was on highlighting uncertainties related to parameter values and model structure. The uncertainty in the meteorological forcing was partly acknowledged by the inclusion of the scaling factors. But, because the scaling factors proved to be among the most sensitive parameters, they could have prevented the identification of an optimal model or patterns relating the parametrization of the models to the lake characteristics, if such an optimal fit exists. A way forward could be to reduce the uncertainty in the meteorological forcing data, and hence hopefully the sensitivity of the scaling factors, by using local meteorological observations instead of reanalysis data.

The sensitivity analysis and cluster analysis could provide hints towards improving global simulations without the need for model-specific calibration. The sensitivity analysis suggests that with parameter values ranges used here, the meteorological forcing data are the most influential in reproducing observed lake water temperatures. Comparing the distributions of best performing parameter values between the lake clusters gives indications on how to scale meteorological forcing (and potentially other, less sensitive parameters) for certain lakes, which could result in an overall improvement in simulating global lake water temperatures. For instance, the models showed clear improvement in model performance when scaling shortwave radiation and

410 wind speed (Figure 7). Sheltering and the cubic scaling of wind speed with mixing may account for some of the need to scale  
wind speed, whereas the scaling of shortwave radiation is less easily explained, though heat transport into the water column,  
shading, or another lack or excess of heat input may play a role. Regardless, an open question remains whether using results of  
the cluster analysis to parametrize uncalibrated simulations should be done. A clear weakness of this study is the low sample  
size in some lake clusters (i.e.  $n = 3$  for “deep” lakes). Also, the model configuration can be problematic, as for instance the  
415 influential  $k_{\min}$  parameter in GOTM had strong effects on mixing and would therefore interact with meteorological scaling  
factors (more details on this can be found in the Supplementary material). Additionally, gridded data are supposed to give the  
best possible estimate of meteorological variables in a certain grid cell. Unless it can be shown that such data are skewed in a  
predictable way for lakes in particular, an adjustment of meteorological variables would mostly be needed to compensate for  
current sub-optimal process descriptions in lake models themselves. So taking the above weaknesses into consideration, these  
420 findings raises the question: Is gridded forcing data adequate to replicate lake-specific meteorological conditions and thus can  
be used to reproduce lake thermal structure? And if so, should improvements in current model performance be found solely in  
improving hydrodynamic process descriptions?

## 5 Conclusions

We calibrated four different lake temperature models to 73 lakes using bias-corrected reanalysis data as forcing, and estimated  
425 the sensitivity of the calibrated parameters. From the six parameters calibrated for each model, only 2–3 were sensitive. This  
suggests that it can be sufficient to calibrate the models using only a subset of parameters. We achieved good model perfor-  
mances compared to previous studies and underscored that while some of the models were performing better overall, each  
model outperformed the others in at least some lakes. We analyzed four different model performance metrics and for over 90%  
of all lakes, at least two models performed best for different performance metrics. To understand the effect of lake character-  
430 istics on the model performance, we grouped the 73 lakes into five clusters representing different characteristics. We highlight  
that both model structure and lake clusters were influencing model performance. In general, the three 1D lake models (GLM,  
GOTM, Simstrat) performed better than the 0.5D model (FLake). More specifically, Simstrat performed better at simulating  
water temperature at the depth of the thermocline than the other models. We attribute this to the seiche module included in  
Simstrat. From these findings we conclude:

- 435 1. There is still room to improve model structure and process description of the 0.5D/1D lake temperature models. Es-  
pecially (better) representation of deep-mixing processes, e.g., internal seiches, could potentially benefit simulations  
results.
2. Using an ensemble of multiple lake models is beneficial, especially as for these 1D (0.5D) models the computational  
cost of using multiple models simultaneously is low. But, there is still room to further take advantage of the ensemble  
440 approach, e.g. by exploring weighted ensemble averaging techniques.

3. Even though we saw patterns in the best performing parameter sets regarding the lake clusters, it is unclear if using this approach might improve uncalibrated simulations (i.e. simulations where no observations are available). This is mainly caused by the fact that we used gridded forcing data, and meteorological scaling factors (wind speed, shortwave radiation) was most influential on lake thermal structure which probably represent the importance of local orography and potential sheltering.

445

These conclusions serve as a baseline for understanding model sensitivity, and can support further improvements and developments of water temperature simulations and, thus, a better assessment of global change in lakes and reservoirs. Additionally, these conclusions can be the basis of a broader discussion about model uncertainty — especially when using gridded forcing data — and its relation to model design and parametrization.

## 450 References

- Andersen, T. K., Bolding, K., Nielsen, A., Bruggeman, J., Jeppesen, E., and Trolle, D.: How morphology shapes the parameter sensitivity of lake ecosystem models, *Environmental Modelling & Software*, 136, 104945, <https://doi.org/10.1016/j.envsoft.2020.104945>, 2021.
- Audet, J., Neif, E. M., Cao, Y., Hoffmann, C. C., Lauridsen, T. L., Larsen, S. E., Søndergaard, M., Jeppesen, E., and Davidson, T. A.: Heat-wave effects on greenhouse gas emissions from shallow lake mesocosms, *Freshwater Biology*, 62, 1130–1142, <https://doi.org/10.1111/fwb.12930>, 2017.
- 455 Ayala, A. I., Moras, S., and Pierson, D. C.: Simulations of future changes in thermal structure of Lake Erken: proof of concept for ISIMIP2b lake sector local simulation strategy, *Hydrology and Earth System Sciences*, 24, 3311–3330, <https://doi.org/https://doi.org/10.5194/hess-24-3311-2020>, 2020.
- Borgonovo, E.: A new uncertainty importance measure, *Reliability Engineering & System Safety*, 92, 771–784, <https://doi.org/10.1016/j.ress.2006.04.015>, 2007.
- 460 Borgonovo, E., Lu, X., Plischke, E., Rakovec, O., and Hill, M. C.: Making the most out of a hydrological model data set: Sensitivity analyses to open the model black-box, *Water Resources Research*, 53, 7933–7950, <https://doi.org/10.1002/2017wr020767>, 2017.
- Bruce, L. C., Frassl, M. A., Arhonditsis, G. B., Gal, G., Hamilton, D. P., Hanson, P. C., Hetherington, A. L., Melack, J. M., Read, J. S., Rinke, K., and et al.: A multi-lake comparative analysis of the General Lake Model (GLM): Stress-testing across a Global Observatory Network, *Environmental Modelling & Software*, 102, 274–291, <https://doi.org/10.1016/j.envsoft.2017.11.016>, 2018.
- 465 Burchard, H., Bolding, K., and Ruiz-Villarreal, M.: GOTM, a general ocean turbulence model. Theory, implementation and test cases, 1999.
- Cengel, Y. A. and Ozisk, M. N.: Solar radiation absorption in solar ponds, *Sol. Energy*, 33, 581–591, 1984.
- Cucchi, M., Weedon, G. P., Amici, A., Bellouin, N., Lange, S., Müller Schmied, H., Hersbach, H., and Buontempo, C.: WFDE5: bias-adjusted ERA5 reanalysis data for impact studies, *Earth System Science Data*, 12, 2097–2120, <https://doi.org/10.5194/essd-12-2097-2020>, 2020.
- 470 Dietze, M. C.: Prediction in ecology: a first-principles framework, *Ecological Applications*, 27, 2048–2060, <https://doi.org/10.1002/eap.1589>, 2017.
- Dirmeyer, P. A., Gao, X., Zhao, M., Guo, Z., Oki, T., and Hanasaki, N.: GSWP-2: Multimodel Analysis and Implications for Our Perception of the Land Surface, *Bulletin of the American Meteorological Society*, 87, 1381–1398, <https://doi.org/10.1175/bams-87-10-1381>, 2006.
- Feldbauer, J., Ladwig, R., Mesman, J. P., Moore, T. N., Zündorf, H., Berendonk, T. U., and Petzoldt, T.: Ensemble of models shows coherent response of a reservoir’s stratification and ice cover to climate warming, *Aquatic Sciences*, 84, 50, <https://doi.org/10.1007/s00027-022-00883-2>, 2022.
- 475 Ford, D. E. and Stefan, H. G.: Thermal predictions using integral energy model, *Journal of the Hydraulics division*, 106, 39–55, <https://doi.org/10.1061/JYCEAJ.0005358>, 1980.
- Frieler, K., Volkholz, J., Lange, S., Schewe, J., Mengel, M., del Rocío Rivas López, M., Otto, C., Reyer, C. P. O., Karger, D. N., Malle, J. T., Treu, S., Menz, C., Blanchard, J. L., Harrison, C. S., Petrik, C. M., Eddy, T. D., Ortega-Cisneros, K., Novaglio, C., Rousseau, Y., Watson, R. A., Stock, C., Liu, X., Heneghan, R., Tittensor, D., Maury, O., Büchner, M., Vogt, T., Wang, T., Sun, F., Sauer, I. J., Koch, J., Vanderkelen, I., Jägermeyr, J., Müller, C., Rabin, S., Klar, J., Vega del Valle, I. D., Lasslop, G., Chadburn, S., Burke, E., Gallego-Sala, A., Smith, N., Chang, J., Hantson, S., Burton, C., Gädeke, A., Li, F., Gosling, S. N., Müller Schmied, H., Hattermann, F., Wang, J., Yao, F., Hickler, T., Marcé, R., Pierson, D., Thiery, W., Mercado-Bettín, D., Ladwig, R., Ayala-Zamora, A. I., Forrest, M., and Bechtold, M.: Scenario setup and forcing data for impact model evaluation and impact attribution within the third round of the Inter-Sectoral Model Intercomparison Project (ISIMIP3a), *Geoscientific Model Development*, 17, 1–51, <https://doi.org/10.5194/gmd-17-1-2024>, 2024.
- 485

- Gaudard, A., Råman Vinnå, L., Bärenbold, F., Schmid, M., and Bouffard, D.: Toward an open access to high-frequency lake modeling and statistics data for scientists and practitioners – the case of Swiss lakes using Simstrat v2.1, *Geoscientific Model Development*, 12, 3955–3974, <https://doi.org/https://doi.org/10.5194/gmd-12-3955-2019>, 2019.
- 490 Giorgi, F. and Mearns, L. O.: Calculation of Average, Uncertainty Range, and Reliability of Regional Climate Changes from AOGCM Simulations via the “Reliability Ensemble Averaging” (REA) Method, *Journal of Climate*, 15, 1141–1158, [https://doi.org/10.1175/1520-0442\(2002\)015<1141:COAURA>2.0.CO;2](https://doi.org/10.1175/1520-0442(2002)015<1141:COAURA>2.0.CO;2), publisher: American Meteorological Society Section: Journal of Climate, 2002.
- Golub, M., Thiery, W., Marcé, R., Pierson, D., Vanderkelen, I., Mercado-Bettin, D., Woolway, R. I., Grant, L., Jennings, E., Kraemer, B. M., Schewe, J., Zhao, F., Frieler, K., Mengel, M., Bogomolov, V. Y., Bouffard, D., Côté, M., Couture, R.-M., Debolskiy, A. V., Droppers, B., 495 Gal, G., Guo, M., Janssen, A. B. G., Kirillin, G., Ladwig, R., Magee, M., Moore, T., Perroud, M., Piccolroaz, S., Raaman Vinnå, L., Schmid, M., Shatwell, T., Stepanenko, V. M., Tan, Z., Woodward, B., Yao, H., Adrian, R., Allan, M., Anneville, O., Arvola, L., Atkins, K., Boegman, L., Carey, C., Christianson, K., de Eyto, E., DeGasperi, C., Grechushnikova, M., Hejzlar, J., Joehnk, K., Jones, I. D., Laas, A., Mackay, E. B., Mammarella, I., Markensten, H., McBride, C., Özkundakci, D., Potes, M., Rinke, K., Robertson, D., Rusak, J. A., Salgado, R., van der Linden, L., Verburg, P., Wain, D., Ward, N. K., Wollrab, S., and Zdrovennova, G.: A framework for ensemble 500 modelling of climate change impacts on lakes worldwide: the ISIMIP Lake Sector, *Geoscientific Model Development*, 15, 4597–4623, <https://doi.org/10.5194/gmd-15-4597-2022>, publisher: Copernicus GmbH, 2022.
- Goudsmit, G.-H., Burchard, H., Peeters, F., and Wüest, A.: Application of  $k-\epsilon$  turbulence models to enclosed basins: The role of internal seiches, *Journal of Geophysical Research: Oceans*, 107, 23–1–23–13, <https://doi.org/10.1029/2001JC000954>, 2002.
- Guo, M., Zhuang, Q., Yao, H., Golub, M., Leung, L. R., Pierson, D., and Tan, Z.: Validation and Sensitivity Analysis of a 1-D Lake Model 505 Across Global Lakes, *Journal of Geophysical Research: Atmospheres*, 126, <https://doi.org/10.1029/2020jd033417>, 2021.
- Guseva, S., Bleninger, T., Jöhnk, K., Polli, B. A., Tan, Z., Thiery, W., Zhuang, Q., Rusak, J. A., Yao, H., Lorke, A., and Stepanenko, V.: Multimodel simulation of vertical gas transfer in a temperate lake, *Hydrology and Earth System Sciences*, 24, 697–715, <https://doi.org/10.5194/hess-24-697-2020>, publisher: Copernicus GmbH, 2020.
- Herman, J. and Usher, W.: SALib: An open-source Python library for Sensitivity Analysis, *The Journal of Open Source Software*, 2, 510 <https://doi.org/10.21105/joss.00097>, 2017.
- Hipsey, M. R., Bruce, L. C., Boon, C., Busch, B., Carey, C. C., Hamilton, D. P., Hanson, P. C., Read, J. S., de Sousa, E., Weber, M., and Winslow, L. A.: A General Lake Model (GLM 3.0) for linking with high-frequency sensor data from the Global Lake Ecological Observatory Network (GLEON), *Geoscientific Model Development*, 12, 473–523, <https://doi.org/10.5194/gmd-12-473-2019>, 2019.
- Hipsey, M. R., Gal, G., Arhonditsis, G. B., Carey, C. C., Elliott, J. A., Frassl, M. A., Janse, J. H., de Mora, L., and Robson, B. J.: A 515 system of metrics for the assessment and improvement of aquatic ecosystem models, *Environmental Modelling & Software*, 128, 104697, <https://doi.org/10.1016/j.envsoft.2020.104697>, 2020.
- Huisman, J., Codd, G. A., Paerl, H. W., Ibelings, B. W., Verspagen, J. M. H., and Visser, P. M.: Cyanobacterial blooms, *Nature Reviews Microbiology*, 16, 471–483, <https://doi.org/10.1038/s41579-018-0040-1>, 2018.
- Håkanson, L.: Models to predict Secchi depth in small glacial lakes, *Aquatic Sciences*, 57, 31–53, <https://doi.org/10.1007/BF00878025>, 520 1995.
- Iwanaga, T., Usher, W., and Herman, J.: Toward SALib 2.0: Advancing the accessibility and interpretability of global sensitivity analyses, *Socio-Environmental Systems Modelling*, 4, 18155, <https://doi.org/10.18174/sesmo.18155>, 2022.
- Jachner, S., Boogaart, K. G. v. d., and Petzoldt, T.: Statistical Methods for the Qualitative Assessment of Dynamic Models with Time Delay (R Package qualV), *Journal of Statistical Software*, <https://doi.org/10.18637/jss.v022.i08>, 2007.

- 525 Jane, S. F., Mincer, J. L., Lau, M. P., Lewis, A. S. L., Stetler, J. T., and Rose, K. C.: Longer duration of seasonal stratification contributes to widespread increases in lake hypoxia and anoxia, *Glob Chang Biol*, 29, 1009–1023, <https://doi.org/10.1111/gcb.16525>, 2023.
- Jansen, J., Woolway, R. I., Kraemer, B. M., Albergel, C., Bastviken, D., Weyhenmeyer, G. A., Marce, R., Sharma, S., Sobek, S., Tranvik, L. J., Perroud, M., Golub, M., Moore, T. N., Raman Vinna, L., La Fuente, S., Grant, L., Pierson, D. C., Thiery, W., and Jennings, E.: Global increase in methane production under future warming of lake bottom waters, *Global Change Biology*, 28, 5427–5440, <https://doi.org/10.1111/gcb.16298>, 2022.
- 530 Kakouei, K., Kraemer, B. M., Anneville, O., Carvalho, L., Feuchtmayr, H., Graham, J. L., Higgins, S., Pomati, F., Rudstam, L. G., Stockwell, J. D., Thackeray, S. J., Vanni, M. J., and Adrian, R.: Phytoplankton and cyanobacteria abundances in mid-21st century lakes depend strongly on future land use and climate projections, *Global change biology*, 27, 6409–6422, <https://doi.org/10.1111/gcb.15866>, 2021.
- Kattel, G. R.: Climate warming in the Himalayas threatens biodiversity, ecosystem functioning and ecosystem services in the 21st century: is there a better solution?, *Biodiversity and Conservation*, 31, 2017–2044, <https://doi.org/10.1007/s10531-022-02417-6>, 2022.
- 535 Khorashadi Zadeh, F., Nossent, J., Sarrazin, F., Pianosi, F., van Griensven, A., Wagener, T., and Bauwens, W.: Comparison of variance-based and moment-independent global sensitivity analysis approaches by application to the SWAT model, *Environmental Modelling & Software*, 91, 210–222, <https://doi.org/10.1016/j.envsoft.2017.02.001>, 2017.
- Kim, H.: Global soil wetness project phase 3 atmospheric boundary conditions (experiment 1), 2017.
- 540 Kitaigorodskii, S. A. and Miropolsky, Y. Z.: On the theory of the open ocean active layer, *Izv. Akad. Nauk SSSR. Fizika Atmosfery i Okeana*, 6, 178–188, 1970.
- Knoll, L. B., Sharma, S., Denfeld, B. A., Flaim, G., Hori, Y., Magnuson, J. J., Straile, D., and Weyhenmeyer, G. A.: Consequences of lake and river ice loss on cultural ecosystem services, *Limnology and Oceanography Letters*, 4, 119–131, <https://doi.org/10.1002/lol2.10116>, 2019.
- 545 Koenings, J. P. and Edmundson, J. A.: Secchi disk and photometer estimates of light regimes in Alaskan lakes: Effects of yellow color and turbidity, *Limnology and Oceanography*, 36, 91–105, <https://doi.org/10.4319/lo.1991.36.1.0091>, 1991.
- Ladwig, R., Rock, L. A., and Dugan, H. A.: Impact of salinization on lake stratification and spring mixing, *Limnology and Oceanography Letters*, 8, 93–102, <https://doi.org/10.1002/lol2.10215>, 2023.
- Lange, S.: Trend-preserving bias adjustment and statistical downscaling with ISIMIP3BASD (v1.0), *Geoscientific Model Development*, 12, 3055–3070, <https://doi.org/10.5194/gmd-12-3055-2019>, 2019.
- 550 Lange, S., Menz, C., Gleixner, S., Cucchi, M., Weedon, G. P., Amici, A., Bellouin, N., Schmied, H. M., Hersbach, H., Buontempo, C., and Cagnazzo, C.: WFDE5 over land merged with ERA5 over the ocean (W5E5 v2.0), <https://doi.org/10.48364/ISIMIP.342217>, 2021.
- Mallard, M. S., Nolte, C. G., Bullock, O. R., Spero, T. L., and Gula, J.: Using a coupled lake model with WRF for dynamical downscaling, *Journal of Geophysical Research: Atmospheres*, 119, 7193–7208, <https://doi.org/10.1002/2014JD021785>, 2014.
- 555 Mckay, M. D., Beckman, R. J., and Conover, W. J.: A Comparison of Three Methods for Selecting Values of Input Variables in the Analysis of Output From a Computer Code, *Technometrics*, 42, 55–61, <https://doi.org/10.1080/00401706.2000.10485979>, 2000.
- Mironov, D. V.: Parameterization of lakes in numerical weather prediction. Part 1: Description of a lake model, German Weather Service, Offenbach am Main, Germany, 2005.
- Mironov, D. V.: Parameterization of lakes in numerical weather prediction. Description of a lake model, Technical Report 11, Deutscher Wetterdienst, Offenbach am Main, Germany, 2008.
- 560



- Moore, T. N., Mesman, J. P., Ladwig, R., Feldbauer, J., Olsson, F., Pilla, R. M., Shatwell, T., Venkiteswaran, J. J., Delany, A. D., Dugan, H., Rose, K. C., and Read, J. S.: LakeEnsemblR: An R package that facilitates ensemble modelling of lakes, *Environmental Modelling & Software*, 143, 105 101, <https://doi.org/10.1016/j.envsoft.2021.105101>, 2021.
- 565 O'Reilly, C. M., Sharma, S., Gray, D. K., Hampton, S. E., Read, J. S., Rowley, R. J., Schneider, P., Lenters, J. D., McIntyre, P. B., Kraemer, B. M., Weyhenmeyer, G. A., Straile, D., Dong, B., Adrian, R., Allan, M. G., Anneville, O., Arvola, L., Austin, J., Bailey, J. L., Baron, J. S., Brookes, J. D., de Eyto, E., Dokulil, M. T., Hamilton, D. P., Havens, K., Hetherington, A. L., Higgins, S. N., Hook, S., Izmet'eva, L. R., Jöhnk, K. D., Kangur, K., Kasprzak, P., Kumagai, M., Kuusisto, E., Leshkevich, G., Livingstone, D. M., MacIntyre, S., May, L., Melack, J. M., Mueller-Navarra, D. C., Naumenko, M., Noges, P., Noges, T., North, R. P., Plisnier, P.-D., Rigosi, A., Rimmer, A., Rogora, M., Rudstam, L. G., Rusak, J. A., Salmaso, N., Samal, N. R., Schindler, D. E., Schladow, S. G., Schmid, M., Schmidt, S. R., Silow, E., Soyulu,
- 570 M. E., Teubner, K., Verburg, P., Voutilainen, A., Watkinson, A., Williamson, C. E., and Zhang, G.: Rapid and highly variable warming of lake surface waters around the globe, *Geophysical Research Letters*, 42, 10,773–10,781, <https://doi.org/10.1002/2015gl066235>, 2015.
- Piccolroaz, S., Zhu, S., Ladwig, R., Carrea, L., Oliver, S., Piotrowski, A., Ptak, M., Shinohara, R., Sojka, M., Woolway, R.-I., and Zhu, D. Z.: Lake Water Temperature Modeling in an Era of Climate Change: Data Sources, Models, and Future Prospects, *Review of Geophysics*, 62, <https://doi.org/https://doi.org/10.1029/2023RG000816>, 2024.
- 575 Pilla, R. M., Williamson, C. E., Adamovich, B. V., Adrian, R., Anneville, O., Chandra, S., Colom-Montero, W., Devlin, S. P., Dix, M. A., Dokulil, M. T., Gaiser, E. E., Girdner, S. F., Hambright, K. D., Hamilton, D. P., Havens, K., Hessen, D. O., Higgins, S. N., Huttula, T. H., Huuskonen, H., Isles, P. D. F., Joehnk, K. D., Jones, I. D., Keller, W. B., Knoll, L. B., Korhonen, J., Kraemer, B. M., Leavitt, P. R., Lepori, F., Luger, M. S., Maberly, S. C., Melack, J. M., Melles, S. J., Muller-Navarra, D. C., Pierson, D. C., Pislegina, H. V., Plisnier, P. D., Richardson, D. C., Rimmer, A., Rogora, M., Rusak, J. A., Sadro, S., Salmaso, N., Saros, J. E., Saulnier-Talbot, E., Schindler, D. E.,
- 580 Schmid, M., Shimaraeva, S. V., Silow, E. A., Sitoki, L. M., Sommaruga, R., Straile, D., Strock, K. E., Thiery, W., Timofeyev, M. A., Verburg, P., Vinebrooke, R. D., Weyhenmeyer, G. A., and Zadereev, E.: Deeper waters are changing less consistently than surface waters in a global analysis of 102 lakes, *Scientific Reports*, 10, 20 514, <https://doi.org/10.1038/s41598-020-76873-x>, 2020.
- Plischke, E., Borgonovo, E., and Smith, C. L.: Global sensitivity measures from given data, *European Journal of Operational Research*, 226, 536–550, <https://doi.org/10.1016/j.ejor.2012.11.047>, 2013.
- 585 Read, J. S., Winslow, L. A., Hansen, G. J. A., Van Den Hoek, J., Hanson, P. C., Bruce, L. C., and Markfort, C. D.: Simulating 2368 temperate lakes reveals weak coherence in stratification phenology, *Ecological Modelling*, 291, 142–150, <https://doi.org/10.1016/j.ecolmodel.2014.07.029>, 2014.
- Rodi, W.: Turbulence models and their application in hydraulics, International Association for Hydraulic Research (IAHR), Monograph Series, IAHR, Delft, 1984.
- 590 Saltelli, A., Tarantola, S., and Campolongo, F.: Sensitivity Analysis as an Ingredient of Modeling, *Statistical Science*, 15, 377–395, <https://www.jstor.org/stable/2676831>, publisher: Institute of Mathematical Statistics, 2000.
- Scavia, D., Wang, Y.-C., Obenour, D. R., Apostel, A., Basile, S. J., Kalcic, M. M., Kirchoff, C. J., Miralha, L., Muenich, R. L., and Steiner, A. L.: Quantifying uncertainty cascading from climate, watershed, and lake models in harmful algal bloom predictions, *Science of The Total Environment*, 759, 143 487, <https://doi.org/10.1016/j.scitotenv.2020.143487>, 2021.
- 595 Staehr, P. A., Bade, D., Van de Bogert, M. C., Koch, G. R., Williamson, C., Hanson, P., Cole, J. J., and Kratz, T.: Lake metabolism and the diel oxygen technique: state of the science, *Limnology and Oceanography: Methods*, 8, 628–644, <https://doi.org/10.4319/lom.2010.8.0628>, 2010.

- Stepanenko, V., Jöhnk, K. D., Machulskaya, E., Perroud, M., Subin, Z., Nordbo, A., Mammarella, I., and Mironov, D.: Simulation of surface energy fluxes and stratification of a small boreal lake by a set of one-dimensional models, *Tellus A: Dynamic Meteorology and Oceanography*, 66, <https://doi.org/https://doi.org/10.3402/tellusa.v66.21389>, 2014.
- 600 Tan, S.-Q., Guo, H.-F., Liao, C.-H., Ma, J.-H., Tan, W.-Z., Peng, W.-Y., and Fan, J.-Z.: Collocation-analyzed multi-source ensembled wind speed data in lake district: a case study in Dongting Lake of China, *Frontiers in Environmental Science*, 11, <https://doi.org/10.3389/fenvs.2023.1287595>, publisher: Frontiers, 2024.
- Thomas, R. Q., Figueiredo, R. J., Daneshmand, V., Bookout, B. J., Puckett, L. K., and Carey, C. C.: A Near-Term Iterative Forecasting System Successfully Predicts Reservoir Hydrodynamics and Partitions Uncertainty in Real Time, *Water Resources Research*, 56, e2019WR026138, <https://doi.org/10.1029/2019WR026138>, publisher: John Wiley & Sons, Ltd, 2020.
- 605 Umlauf, L., Bolding, K., and Burchard, H.: GOTM – Scientific Documentation, Leibniz-Institute for Baltic Sea Research, <https://gotm.net/portfolio/documentation/>, please check up-to-date version on [www.gotm.net](http://www.gotm.net), 2005.
- Vanderkelen, I., Lipzig, N. P. M. v., Lawrence, D. M., Droppers, B., Golub, M., Gosling, S. N., Janssen, A. B. G., Marcé, R., Schmed, H. M., Perroud, M., Pierson, D., Pokhrel, Y., Satoh, Y., Schewe, J., Seneviratne, S. I., Stepanenko, V. M., Tan, Z., Woolway, R. I., and Thiery, W.: Global Heat Uptake by Inland Waters, *Geophysical Research Letters*, 47, e2020GL087867, <https://doi.org/https://doi.org/10.1029/2020GL087867>, \_eprint: <https://agupubs.onlinelibrary.wiley.com/doi/pdf/10.1029/2020GL087867>, 2020.
- 610 Weber, M., Rinke, K., Hipsey, M., and Boehrer, B.: Optimizing withdrawal from drinking water reservoirs to reduce downstream temperature pollution and reservoir hypoxia, *Journal of Environmental Management*, 197, 96–105, <https://doi.org/10.1016/j.jenvman.2017.03.020>, 2017.
- Weinstock, J.: Energy dissipation rates of turbulence in the stable free atmosphere, *Journal of the Atmospheric Sciences*, 38, 880–883, [https://doi.org/10.1175/1520-0469\(1981\)038<0880:EDROTI>2.0.CO;2](https://doi.org/10.1175/1520-0469(1981)038<0880:EDROTI>2.0.CO;2), 1981.
- Woolway, R. I. and Merchant, C. J.: Worldwide alteration of lake mixing regimes in response to climate change, *Nature Geoscience*, 12, 271–276, <https://doi.org/10.1038/s41561-019-0322-x>, 2019.
- 620 Woolway, R. I., Denfeld, B., Tan, Z., Jansen, J., Weyhenmeyer, G. A., and La Fuente, S.: Winter inverse lake stratification under historic and future climate change, *Limnology and Oceanography Letters*, n/a, <https://doi.org/10.1002/lo12.10231>, \_eprint: <https://onlinelibrary.wiley.com/doi/pdf/10.1002/lo12.10231>, 2021a.
- Woolway, R. I., Sharma, S., Weyhenmeyer, G. A., Debolskiy, A., Golub, M., Mercado-Bettín, D., Perroud, M., Stepanenko, V., Tan, Z., Grant, L., Ladwig, R., Mesman, J., Moore, T. N., Shatwell, T., Vanderkelen, I., Austin, J. A., DeGasperis, C. L., Dokulil, M., La Fuente, S., Mackay, E. B., Schladow, S. G., Watanabe, S., Marcé, R., Pierson, D. C., Thiery, W., and Jennings, E.: Phenological shifts in lake stratification under climate change, *Nature Communications*, 12, 2318, <https://doi.org/10.1038/s41467-021-22657-4>, 2021b.
- 625 Wüest, A. and Lorke, A.: SMALL-SCALE HYDRODYNAMICS IN LAKES, *Annual Review of Fluid Mechanics*, 35, 373–412, <https://doi.org/10.1146/annurev.fluid.35.101101.161220>, publisher: Annual Reviews, 2003.
- 630 Wüest, A., Piepke, G., and Van Senden, D. C.: Turbulent kinetic energy balance as a tool for estimating vertical diffusivity in wind-forced stratified waters, *Limnology and Oceanography*, 45, 1388–1400, <https://doi.org/10.4319/lo.2000.45.6.1388>, 2000.
- Yeates, P. and Imberger, J.: Pseudo two-dimensional simulations of internal and boundary fluxes in stratified lakes and reservoirs, *International Journal of River Basin Management*, 1, 297–319, <https://doi.org/10.1080/15715124.2003.9635214>, 2003.
- Zhuang, Q., Guo, M., Melack, J. M., Lan, X., Tan, Z., Oh, Y., and Leung, L. R.: Current and Future Global Lake Methane Emissions: A Process-Based Modeling Analysis, *Journal of Geophysical Research: Biogeosciences*, 128, <https://doi.org/10.1029/2022jg007137>, 2023.
- 635

*Code and data availability.* The used software LakeEnsemblR is available on GitHub (<https://github.com/aemon-j/LakeEnsemblR>). The scripts to perform the sensitivity analysis, create the plots, and do statistical analysis can be found in this repository <https://zenodo.org/doi/10.5281/zenodo.13150422>. The scripts to set up and run the calibration can be found in this repository <https://zenodo.org/doi/10.5281/zenodo.13165427>. ISIMIP forcing data and the post-calibration climate simulations are available from <https://data.isimip.org/>, and the lake temperature observations and hypsographs can be found at [https://github.com/icra/ISIMIP\\_Local\\_Lakes/tree/main/LocalLakes](https://github.com/icra/ISIMIP_Local_Lakes/tree/main/LocalLakes).

*Author contributions.* JF and JM conceived the idea for this paper, designed and performed model calibrations. JF and TKA performed the sensitivity analysis. All authors analysed model performance and sensitivity analysis results. JF, JM and RL wrote main parts of the manuscript with contributions from TKA. All authors read and reviewed the final version of the manuscript.

*Competing interests.* The authors declare no competing interests.

*Acknowledgements.* This work was conceived at the Global Lake Ecological Observatory Network (GLEON), and benefited from continued participation and travel support from GLEON. We would like to thank Muhammed Shikhani and Lipa Gutani T. Nkwalele for valuable feedback on an earlier version of the manuscript and Tadhg Moore, Thomas Petzoldt, and Martin Schmid for fruitful discussions during the study. JF received funding from the BMBF project FKZ 01LR 2005A—Fördermaßnahme ‘Regionale Informationen zum Klimahandeln’ (RegIKlim). JPM was funded by the European Union’s Horizon 2020 research and innovation programme, under grant agreement No. 101017861 (SMARTLAGOON). TKA was funded by the Grundfos Foundation (Lake Stewardship III).